Model calibration of a variable refrigerant flow system with a dedicated outdoor air system: A case study

Dongsu Kim[1], Sam J. Cox[1], Heejin Cho[1], and Piljae Im[2]*

[1] Mechanical Engineering, Mississippi State University, Starkville, Mississippi 39759
[2] Building Technologies Research and Integration Center, Oak Ridge National Laboratory, TN 37831, USA
*Corresponding author: +1-865-241-2312; imp1@ornl.gov

ABSTRACT

With increased use of variable refrigerant flow (VRF) systems in the U.S. building sector, interests in capability and rationality of various building energy modeling tools to simulate VRF systems are rising. This paper presents the detailed procedures for model calibration of a VRF system with a dedicated outdoor air system (DOAS) by comparing to detailed measured data from an occupancy emulated small office building. The building energy model is first developed based on as-built drawings, and building and system characteristics available. The whole building energy modeling tool used for the study is U.S. DOE's EnergyPlus version 8.1. The initial model is, then, calibrated with the hourly measured data from the target building and VRF-DOAS system. In a detailed calibration procedures of the VRF-DOAS, the original EnergyPlus source code is modified to enable the modeling of the specific VRF-DOAS installed in the building. After a proper calibration during cooling and heating seasons, the VRF-DOAS model can reasonably predict the performance of the actual VRF-DOAS system based on the criteria from ASHRAE Guideline 14-2014. The calibration results show that hourly CV-RMSE and NMBE would be 15.7% and 3.8%, respectively, which is deemed to be calibrated. The whole-building energy usage after calibration of the VRF-DOAS model is 1.9% (78.8 kWh) lower than that of the measurements during comparison period.

KEYWORDS: Variable refrigerant flow, Dedicated outdoor air system, Building simulation, Calibration.

1. INTRODUCTION

1.1 Background and purpose

The building sector accounts for about 40% of the entire energy consumption in the U.S. [1]. The energy consumption used for heating, ventilation and air conditioning (HVAC) systems represents approximately 50% of the total energy usage of the building sector [2]. Variable refrigerant flow (VRF) systems are a well-developed and widely adapted HVAC technology in many Asian and European countries and provide several key benefits, including: energy efficiency, ease of installation, design flexibility, and easy maintenance [3][4][5].

As a VRF system is a still new HVAC technology in the U.S. marketplace, a number of recent studies have attempted to evaluate the energy performance of VRF systems and to identify the benefits of them. Most studies include field or laboratory empirical tests as well as simulation modeling analysis of the system performance or VRF control strategies [6]. Aynur [7] provides a good overview of VRF systems. Based on this detailed review, VRF systems serve high energy savings potential and better indoor thermal

comfort when compared to traditional HVAC systems, such as variable air volume (VAV) and fan coil unit (FCU) systems, due to the operation in the individual control mode.

In terms of energy savings potential of VRF systems, Im and Munk [8] evaluated the energy performance of a multi-split VRF system in comparison to a typical RTU-VAV system installed in the Oak Ridge National Laboratory's Flexible Research Platform (FRP). Their empirical analysis showed energy savings of a VRF system were estimated to be around 20% over a RTU-VAV system during cooling period. Kim et al. [9] compared VRF systems with RTU-VAV systems to evaluate energy savings potential of VRF systems for 16 different climates in the U.S. Simulation results from their comparable study pointed out that VRF systems could save about 15%-42% and 18%-33% for HVAC site and source energy, respectively. Zhou et al. [10] developed a VRF model in EnergyPlus and conducted a comparative study with VAV and FCU systems and showed a VRF system could lower about 11% and 22% HVAC energy consumption, as compared to FCU and VAV systems, respectively. Yu et al. [11] surveyed and measured field data to investigate and compare cooling energy consumption between VAV and VRF systems in typical office buildings in China. Aynur et al. [12] analyzed a comparative study between VRF and VAV systems and evaluated the energy savings potential of VRF systems. Their simulation results showed that VRF systems could consume about 38%-83% less energy usage for cooling season. Based on those comparison studies, it is indicated that VRF systems could offer significant reduction in building energy usage depending on climate, system control, and its operation mode.

As advanced controls offer a variety of operational benefits for energy savings and indoor thermal comfort in buildings [5], many recent studies have developed enhanced control strategies and energy modeling methods of VRF systems that individually operate cooling and heating for each zone [13][14][15][16][17]. Meng et al. [13] experimentally investigated the cooling performance of a multi-split VRF system by employing two different heat exchangers with various part load ratios (PLRs). From their experimental results, it was obtained that a VRF system with the microchannel heat exchanger could provide better thermal comfort to occupants in heating season. Tu et al. [18] developed the control strategy of a VRF system with multi-compressors to ensure stable and reliable operation and high energy efficiency. Choi and Kim [14] evaluated the performance of an inverter-driven multi-air conditioner that consists of multi-indoor units with a compressor operated by an inverter diver with electronic expansion valves (EEVs) under different indoor loads, EEV openings, and compressor speeds. With their experimental results, it was suggested that the superheat points had to be controlled within the optimum value, and compressor speed needed to be adjusted to appropriately modulate the cooling capacities for each indoor unit.

Ventilation is still considered to be one of the main issues with VRF systems since VRF systems only circulate indoor air without any outdoor air (OA) intake to satisfy IAQ in commercial buildings [19][20]. Due to the main drawback with OA supplies, additional ventilation systems, such as a dedicated outdoor air system (DOAS) combined with the heat recovery ventilation (HRV) or additional HVAC systems [16], are essential to be included with the VRF systems to overcome its limitations on providing OA ventilation [21]. Aynur et al. [22] investigated the effects of the ventilation and a control mode on the energy efficiency and indoor thermal comfort of a VRF system. They concluded that a VRF system that operates in the individual control mode for each zone could better serve indoor thermal comfort under both cooling and heating conditions. In addition, a VRF system that configures with a DOAS showed higher energy consumption than the non-ventilated VRF system, mainly due to additional ventilation fans and load. Kim et al. [20] developed a multi-objective optimal control strategy for a VRF system with a DOAS to reduce building energy consumption while fulfilling IAQ as well as thermal and humidity comfort at the same time. Zhu et al. [21] proposed and investigated a new air-conditioning system that combines a VRF system

with a DOAS. They used a validated simulation model to evaluate the performance of the new proposed system, and their results presented a new proposed system that maintained their specific set-points and acceptable IAQ in all zones during the heating period. From the perspective of VRF systems with DOASs, note that VRF systems combined with DOASs tend to consume more energy when compared to those systems without DOASs. A DOAS could also affect indoor thermal comforts and the IAQ, depending on a DOAS operation modes However, there have been still several concerns for the application and analysis of VRF systems with DOASs, such as higher initial cost, lack of familiarity with the technology, and safety issues with refrigerant leakage in the U.S. [3][7].

Modeling of VRF systems has been performed by many researchers in terms of modeling techniques and approaches. Li et al. [23] developed a VRF simulation module for water-cooled VRF in EnergyPlus. They compared their simulated results with measured data from an actual building in China [24], and they showed the mean of the absolute value of the daily error between the simulated and measured results is 11.3% for cooling capacity while the error for compressor power is 15.7% in the 9 days. Shen. et al [25] developed a detailed steady-state multi-split VRF model using TRNSYS. Their simulated results showed good agreement in both cooling and heating EERs of multiple units in comparison with measured data, obtained from product literature. Raustad [26] introduced a VRF HP simulation model in EnergyPlus, which was an empirical equation fit model based on manufacturers' performance data. Based on a VRF HP simulation model in the reference [26], Sharma and Raustad [27] validated against field data measured at an multi-zone building. It was found that about 72% of all the simulated energy use fall within 25% of the measured data, and a coefficient of variation of the root mean square error, CV (RMSE), was about 21% between measured and simulated total energy use. Hong et al. [28] developed a new physics based VRF simulation module in EnergyPlus version 8.4. With their comparison between measured and simulated results, normalized mean bias errors (NMBEs) were 2.8% and 4.5% for cooling and heating operations. They also mentioned that a new VRF model offered the benefits of enabling advanced controls and improving accurate energy prediction for VRF systems.

The calibration of building energy models with measured data is essential to accurately predict energy savings potential because of the considerable uncertainty involved with various input parameters used in such building energy modeling [29][30]. Clarke et al. [31] first classified a calibration approach into several ways (i.e., manual, iterative, and pragmatic intervention) according to the selection and justification of the interventions. Based on this classification, Reddy [30] gives a good review of calibration approaches to building energy modeling: (1) calibration based on manual, iterative, and pragmatic intervention, (2) calibration based on a suite of informative graphical comparative displays, (3) calibration based on special tests and analytical procedures, and (4) analytical/mathematical methods of calibration. Then, these classifications were further extended by Coakely et al. [32], and current calibration approaches can be more broadly assorted with manual and automated. Manual approaches basically depend on iterative pragmatic intervention by tuning refining input parameters in a heuristic manner based on the experience and expertise of the modeler. In contrast with manual calibrations, automated approaches are based on mathematical and statistical techniques (i.e., not modeler driven) to minimize errors by input parameters and calibrate building energy modeling.

Numerous studies have shown building model calibration within many building related applications using manual and automated approaches [33][34][29][35][36][37][38][39]. Raftery et al. [33] used a systematic and evidence-based methodology in manual approaches to calibrate the whole building energy modeling. They turned out that this approach improved the reliability and accuracy of the calibration process with the final model by keeping a history of the decisions and reducing the likelihood of analysts

tuning input parameters. Sun et al. [39] introduced a new automated model calibration approach using graphical pattern identification by logic linking parameter. Based on their results, although there are still some limitations to this approach, the pattern-based automated calibration methodology can be useful to remove any need for manual input or long computation time compared to traditional calibration process. For VRF systems in buildings, a detailed calibration and its methods specifically for the whole buildings have been rarely studied in literature. Shen and Rice [40] developed a VRF system model that consists of five indoor units and one outdoor unit and manually calibrated their model against a manufacturer's product literature. Yun and Song [41] introduced a new automatic calibration method for a VRF system to accurately predict building energy consumption. However, a detailed calibration approach for an entire building with VRF and DOAS systems has not been presented in literature.

The objective of this paper is to present the detailed procedures for the model calibration of a VRF-DOAS that can improve the overall accuracy of the building energy modeling. Accurate modeling of VRF system performance in real buildings is critical for better understanding of the benefit of VRF system and evaluating performance of the model in different climate environments. In this study the model calibration is performed based on data collected from an experimental facility developed by Oak Ridge National Laboratory (ORNL), called Flexible Research Platform (FRP). The initial building energy model reflects basic building information available from the manufacturers' data sheets and default HVAC input values that EnergyPlus typically offers for a typical VRF system. In the calibration procedures, the original EnergyPlus code is modified to correctly model the installed VRF-DOAS in FRP. Then building energy modeling is manually calibrated based on the criteria from ASHRAE Guideline 14-2014 [42] by comparing to the measured data from the FRP under cooling and heating periods.

2. TARGET BUILDING DESCRIPTION

2.1 A test facility: two-story flexible research platform (FRP)

The two story flexible research platform (FRP) facility is a two-story, 3,200 ft^2 (297.3 m^2) multi-zone building. The FRP is an occupancy emulated research building that represents a typical existing low-rise, a small office building common in the U.S. (Figure 1 (a)). For this study, since human interference is one of the main factors for uncertainty in building energy use, the occupancy in the FRP is emulated so that such uncertainty in calibration process is attributable only to system performance and weather. To emulate a fixed occupancy, lighting and other internal loads were controlled with preprogrammed portable heaters for sensible heat gains and humidifiers for latent heat gains. On this building, detailed building activities such as building envelope retrofits, addition of alternative building components, and any HVAC system changes were logged and carried out. The building system's performance, such as electric energy consumption and temperature, was also closely monitored. The collected data was used to model and calibrate the VRF-DOAS simulation model. In addition, a dedicated weather station was installed on the roof (Figure 1 (e)). The data gathered from the weather station is used to pack a weather file that can be used in the modeling and the calibration procedures. The VRF system installed in the FRP is a 12-ton (42 kW) heat pump type system with a DOAS (Figure 1 (c)) and contains two scroll compressors charged with R-410a (Figure 1 (b) and (d)). Table 1 summarizes the FRP and the VRF system characteristics [6].

Figure 1. The test facility: (a) two-story flexible research platform, (b) VRF outdoor unit, (c) DOAS unit, (d) one of VRF indoor units, and (e) dedicated weather station on the FRP.

Table 1. Building characteristics of two-story flexible research platform (FRP)

Location	Oak Ridge, Tennessee, USA
Building size	Two-story, 12.2×12.2 m (40×40 ft), 4.3 m (14 ft) floor-to-floor height
Exterior walls	Concrete masonry units with face brick, RUS-11 (RSI-1.9) fiberglass insulation
Floor	Slab-on-grade
Roof	Metal deck with RUS –18(RSI –3.17) polyisocyanurate insulation
Windows	Double-pane clear glazing, 28% window-to-wall ratio
Baseloads	9.18W/m² (0.85 W/ft²) lighting power density, 14.04W/ m² (1.3 W/ft²) equipment power density
VRF system capacity	42 kW (12 ton) VRF system with a DOAS

VRF refrigerant pipe	Fareast equivalent length: 31.0 m (101.7 ft), the highest height: 8.6 m (28.2 ft)

2.2 Variable refrigerant flow with dedicated outdoor air system (VRF-DOAS)

The VRF system installed at FRP has an outdoor unit, one DOAS unit, and ten indoor units with capacities ranging from 1.8 to 5.3 kW (0.5–1.5 tons) as shown in Figure 2. The system capacity of the corresponding indoor and outdoor units was chosen based on the load calculations from Manual N [43]. As seen in Figure 2, the ten indoor units and the DOAS are connected to the same VRF outdoor condensing unit, and the DOAS provides conditioned OA to ten thermal zones. In addition, the OA requirement for the FRP building was estimated according to the ASHRAE Standard 62.1-2013 [19]. Note that the VRF system in this study can only provide cooling or heating at a single time and cannot provide simultaneous heating and cooling for different thermal zones.

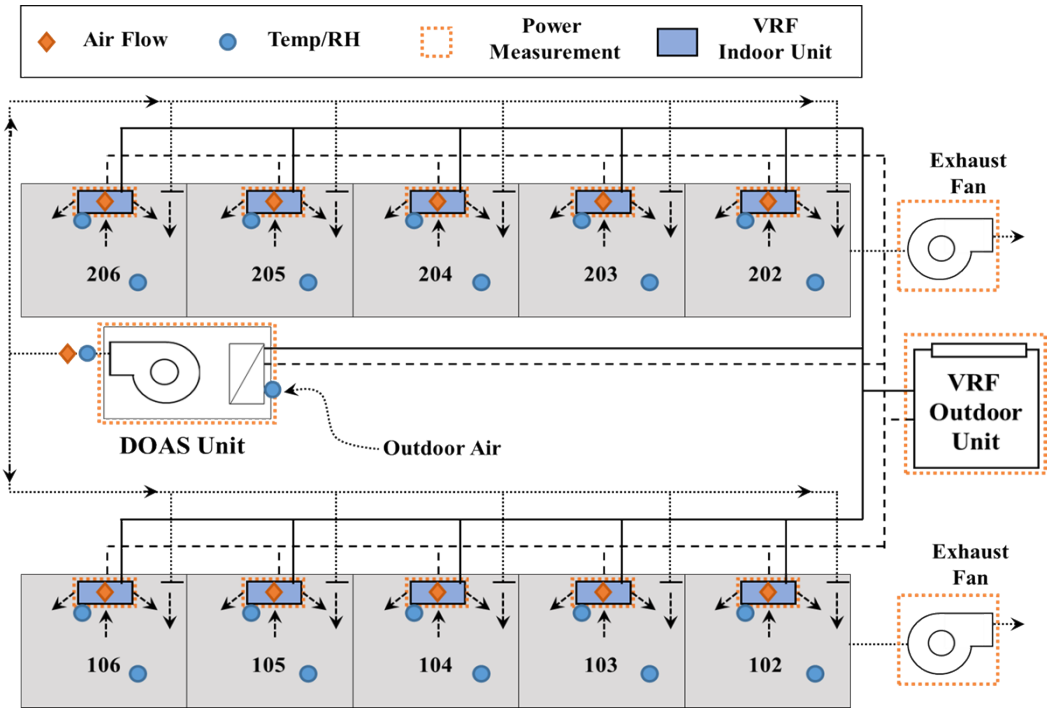

Figure 2. The VRF-DOAS schematic installed in FRP

During the test period (i.e., July 11, 2015 through March 6, 2016), there were several other tests ongoing with different types of HVAC systems at the FRP. Therefore, only the days when the VRF system fully conditioned the FRP were selected for the model calibration. Those are 6 days during August 15, 2015 through September 20, 2015 for cooling season, and 19 days during October 10, 2015 through February 19, 2016 for heating season.

The measured data for the VRF system includes:

1) Continuous inlet/outlet air flow, temperature, humidity measurement for each indoor unit of VRF system,
2) One-time airflow measurements for each indoor unit of VRF system,
3) Continuous inlet/outlet air flow, temperature, humidity measurement for the DOAS,
4) and power consumption for the VRF outdoor unit, each VRF indoor unit, and the DOAS (Im et al. 2015).

Note that airflow for each indoor unit was measured only once because indoor units were operated at fixed flow rates.

3. CALIBRATION APPROACHES

Recent calibration approaches of building energy modeling require the use of hourly or monthly data for a certain period of time in order to improve the accuracy of building dynamics (in terms of diurnal scheduling and HVAC equipment control) [30][35]. ASHRAE Guideline 14-2014 [42] summarizes the methodology and several calibration steps to effectively calibrate and estimate the building energy savings associated with measured data. Based on this guideline and literature reviews, an evidence-based methodology in manual approaches is adopted to properly model and calibrate the VRF-DOAS system installed at the FRP [33].

The following steps are performed in this study: (1) modification of the existing EnergyPlus v8.1 source code to enable modeling of the physical settings of the VRF-DOAS described in the previous section, (2) after modeling the building envelope and HVAC system, calibration of building envelope model and internal heat gain inputs to ensure that the simulated delivered cooling and heating loads are comparable with the measured data and (3) calibration of VRF-DOAS model for the total building energy consumption based on the definition from ASHRAE Guideline 14-2014 [42].

3.1 Step 1: EnergyPlus source code modification

EnergyPlus 8.1 allows for performance curve based quasi-steady state simulation of VRF systems. The EnergyPlus 8.1 source code is modified to model the current VRF-DOAS setting in the FRP; particularly the usage of VRF heating and cooling coils to condition OA in the DOAS described in the previous section. The original version 8.1 of EnergyPlus uses an OA mixer object or air-loop DOASs with separated HVAC coils, such as a single or two speed DX coil for a VRF model with a DOAS [44][45]. Therefore, the EnergyPlus 8.1 source code is modified to allow for OA to be provided through an air-loop DOAS directly to individual zones while being conditioned with VRF heating and cooling coils connected to the outdoor unit. EnergyPlus has three stages of simulation: Zone load calculations, air loop calculations, and zone equipment calculations. This requires the data from VRF coils simulated in the air loop stage to be passed to the zonal equipment stage and then be aggregated with the zone VRF coil capacities. Thereafter, the VRF outdoor unit is simulated with steady state performance curves to calculate electric energy usage. If the capacity of the outside unit is exceeded, the air loop VRF coil is assumed to have priority, and the zonal coil capacities are systematically reduced until the capacity is no longer exceeded.

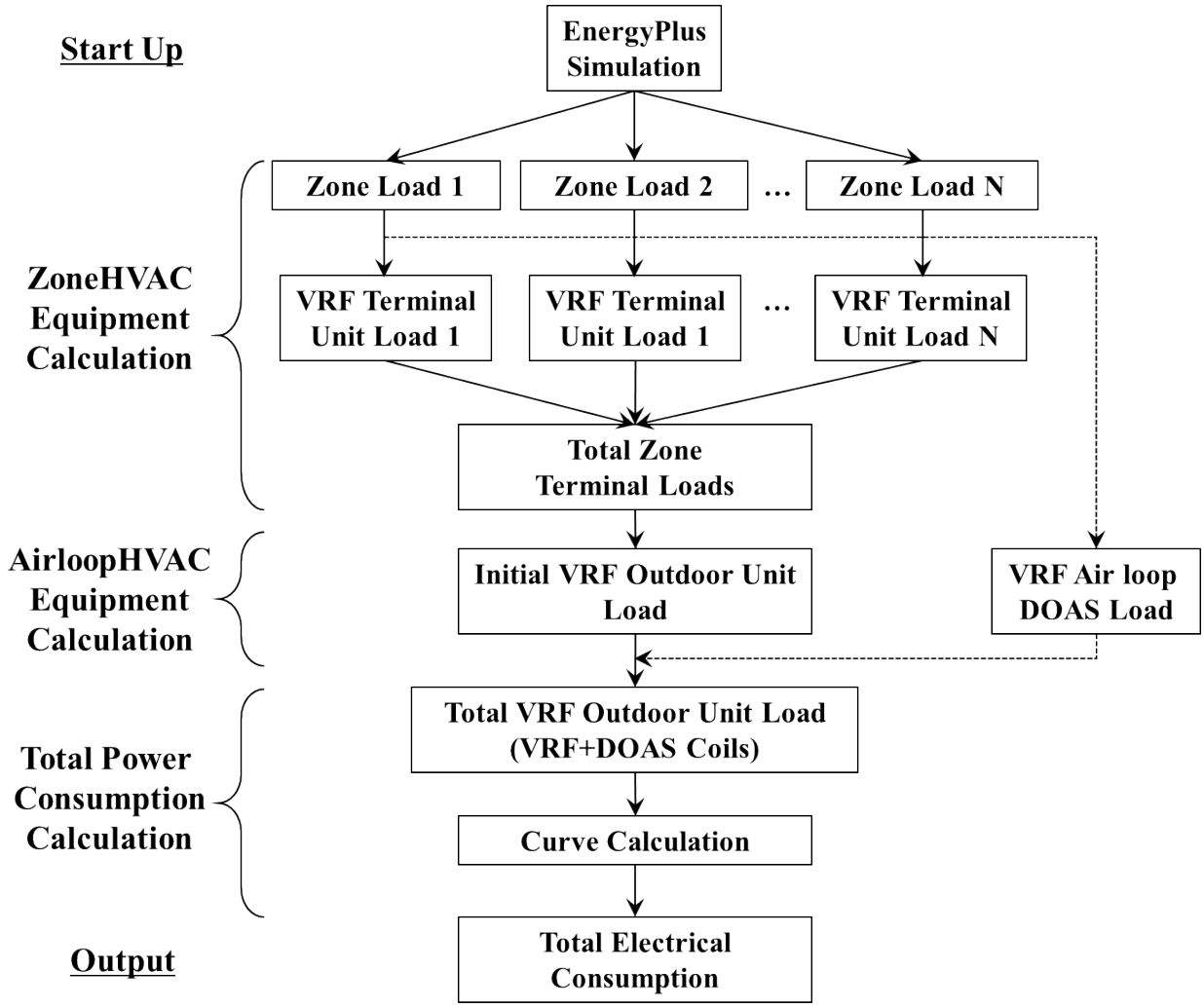

Figure 3. Process of the modified EnergyPlus version 8.1 for the VRF-DOAS

With this source code modification, two new objects, VRF air-loop cooling and heating coils (object names Coil: Cooling: DX: VRFAirloop and Coil: Heating: DX: VRFAirloop) shown in Figure 4, were added to enable a DOAS system coupled with a VRF outdoor unit to provide 100% conditioned OA to individual zones, as illustrated in Figure 2. Figure 3 demonstrates the simulation process of the modified EnergyPlus version. The new VRF air-loop coil objects are modeled to calculate the coil performance based on performance curves in the same manner compared to the single-speed DX heating and cooling coils modeled in EnergyPlus 8.1 [44]. The coil capacities are accounted into the VRF condenser calculations along with the average inlet wet-bulb conditions for each coil linked to the VRF condenser. In the current modification, the model uses performance information at rated conditions along with curve fits for variations in total capacity, energy input ratio, and part-load fraction to determine the performance of the unit at part-load conditions.

Figure 4 shows new objects and their connections in modified version of EnergyPlus. The VRF air loop coils are stand-alone objects that the VRF outdoor unit searches for during the outdoor unit calculations.

As such, any configuration of an air loop that can be connected to a single speed DX coil is valid for the VRF air loop coil. It can be connected to the branch object that further extends to several component objects, including heating/cooling DX coils, the variable volume fan, and the outdoor air controller throughout the air loop HVAC. All operation options that the air loop HVAC in EnergyPlus provides can be used, such as economizer and mechanical ventilation controls.

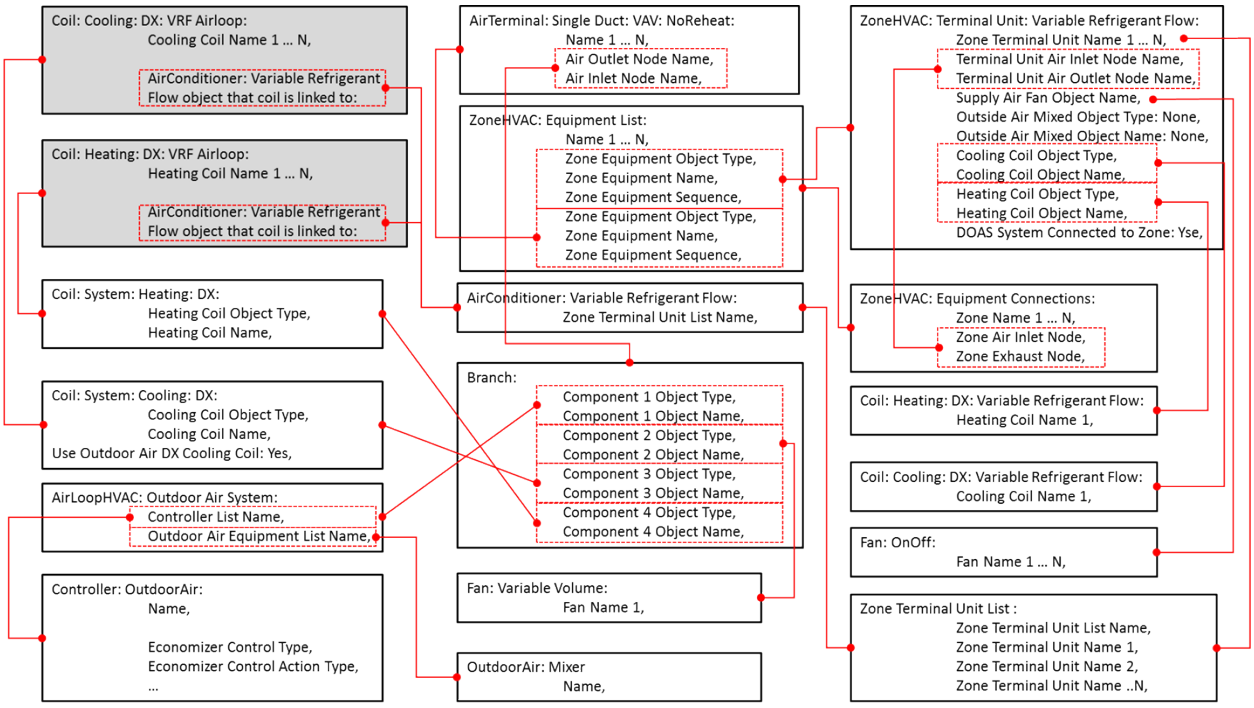

Figure 4. Modified VRF-DOAS objects and their connections in modified version of EnergyPlus (modified from [44])

In this modification process, manufacturers' data in the EnergyPlus VRF HP model [44][26] are used for the coefficients of performance curves. After the source code modification, the new EnergyPlus executable file and input data dictionary (idd) file were generated and made available to model the VRF-DOAS system installed in the FRP. A schematic diagram of the VRF-DOAS for a single-zone in the modified version of EnergyPlus is illustrated in Figure 5 (b).

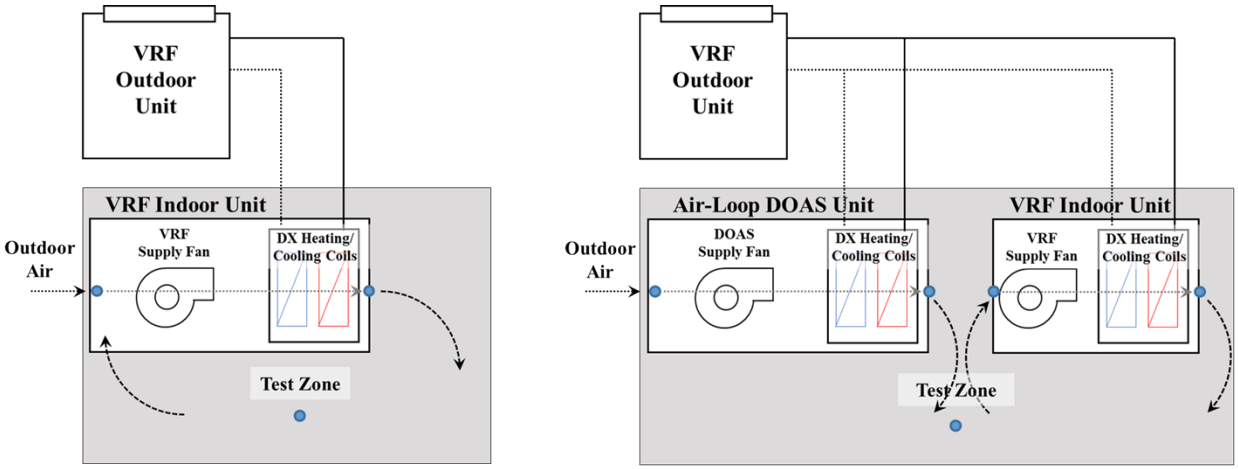

Figure 5. Two schematic diagrams of VRF systems in a single test zone for validation: (a) the original and (b) the modified version of EnergyPlus

To check the validity of the modified version of EnergyPlus 8.1, a simulation test is performed with a single-zone building model. Two single-zone building models for each version of EnergyPlus are placed in the same ambient conditions, and two different VRF systems are modeled in each version of EnergyPlus as shown in Figure 5: a VRF terminal unit with an OA mixer for the original EnergyPlus (VRF+OAmixer) and a VRF terminal unit with an air-loop DOAS for the modified version of EnergyPlus (VRF+Airloop DOAS). The identical weather file (i.e., USA TN Knoxville –McGhee-TMY3.epw) is used to compare two different VRF models with OA; it is for a summer period in July and a winter period in January.

For validation, three main outputs (i.e., DX heating and cooling coils' rate, VRF heat pump heating and cooling rate, and VRF heat pump electrical energy use) of a VRF system in VRF+Airloop is compared with VRF+OAmixer, as illustrated in Figure 6 through Figure 8. Heating and cooling rates of each coil in the VRF+Airloop model, shown in Figure 6, typically reflect heating and cooling rates from both a terminal VRF indoor unit and the air-loop DOAS unit, as Figure 5 shows.

From the comparison of each output data between the VRF+OAmixer and the VRF+Airloop models, Figure 6 through Figure 8 indicate that simulated VRF energy usage from each version of EnergyPlus tends to agree for the cooling period, while the VRF+Airloop model presents slightly more heating rate and energy usage than the VRF+OAmixer model for heating period. That is expected because in the modified model, the zone and OA loads are removed separately using the terminal VRF and the air-loop DOAS with a VRF coil; whereas the original model removes the zone and OA loads simultaneously by mixing OA and return air from the zone and by using a single VRF coil to remove the mixed total heating energy. As two systems provide heating and cooling in the modified model, it has a tendency to overheat or overcool the zone because two units may try to provide heating and cooling at the same time separately to the zone. This issue was also observed in measured data.

Overall, when the perspective of the coefficients of determination (R^2) is considered in three different comparisons, strong linear relationships between the VRF+OAmixer and the VRF+Airloop models are shown in all figures. This indicates that the modified version of EnergyPlus not only enables to model the air-loop DOAS connected with a VRF outdoor unit, but it also reasonably predicts electrical energy use from a VRF HP system while providing conditioned OA to individual zones at the same time.

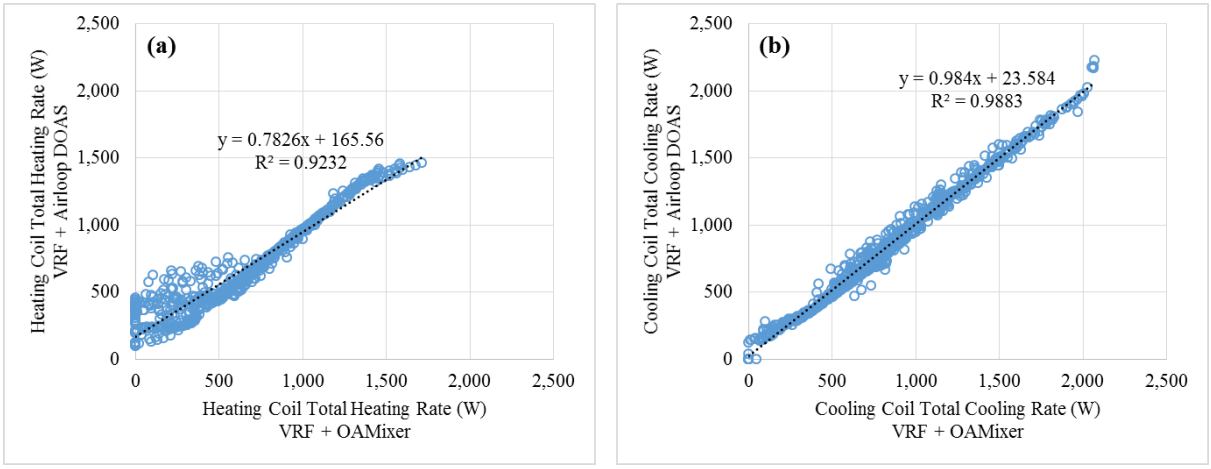

Figure 6. Cross plots of each coil total cooling and heating rate between the original and modified version models: (a) heating period and (b) cooling period

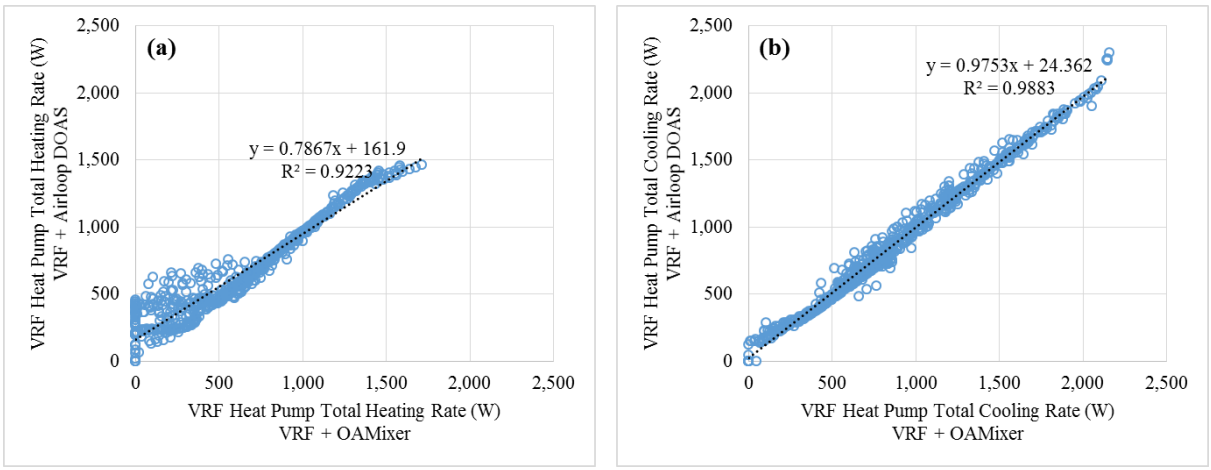

Figure 7. Cross plots of VRF heat pump total heating and cooling rate between the original and modified version models: (a) heating period and (b) cooling period

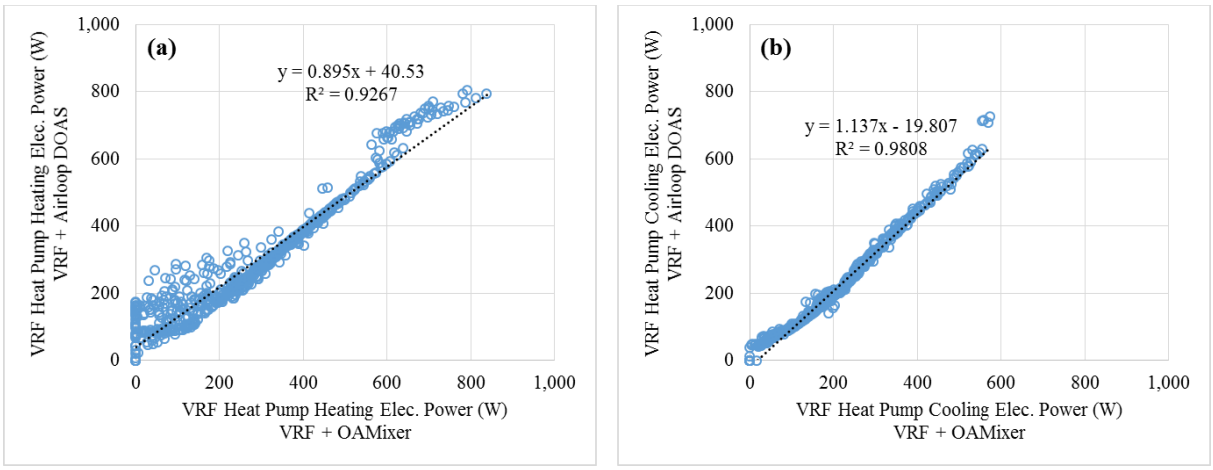

Figure 8. Scatter plots of VRF heat pump total heating and cooling electrical power between the original and modified version models: (a) heating period and (b) cooling period

3.2 Step 2: Calibration 1 – Building load calibration

As a first step of a detailed calibration in this study, the building's simulated delivered cooling and heating loads are compared with the calculated delivered heating and cooling loads based on the air side measured data for VRF indoor units and the DOAS unit as presented in Figure 2. In a typical calibration procedure, this step might not be possible as the delivered cooling and heating loads for a specific building would not be readily available. As simulated whole building energy use is usually compared to the measured one without considering this step, the typical calibration cannot eliminate a coincidental event that lower building loads would be offset by higher HVAC energy use (or vice versa).

Building envelope model, first, is calibrated by modifying the input values for the categories shown below.

1) Weather data
2) Infiltration
3) Interior light intensity and schedule
4) Plug load intensity and schedule

Actual weather data from the dedicated weather station is collected and used to pack weather data file for EnergyPlus.

For infiltration updates, a blower door test was performed to measure the airtightness of the FRP. The measurement is used to calculate the infiltration value for the FRP building model in EnergyPlus based on an infiltration calculation method [46]. 2.33 $m^3/s\text{-}m^2$ is put on "flow per exterior surface area" input in EnergyPlus for all exterior zone surfaces.

The intensities and schedules of the interior lights and equipment values (plug load) are also manually updated based on the measured lighting and plug loads in the FRP. Figure 9 shows the output trends of the interior lights after modification in the EnergyPlus model. The interior lights shown in Figure 9 are hourly average values in EnergyPlus shown in terms of the electric energy for ten zones for seven representative days during the measurement period. Figure 10 shows comparison of the interior plug load for the measured and the simulated data after updates in EnergyPlus. The interior plugs provided in Figure 10 are also hourly

average values in EnergyPlus for all ten zones for seven representative days during the entire comparison period.

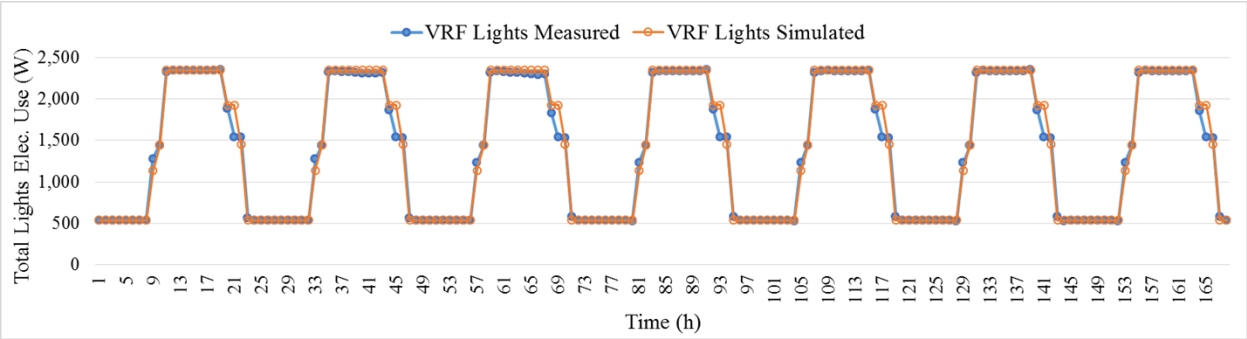

Figure 9. Hourly interior lights electricity use for typical seven days

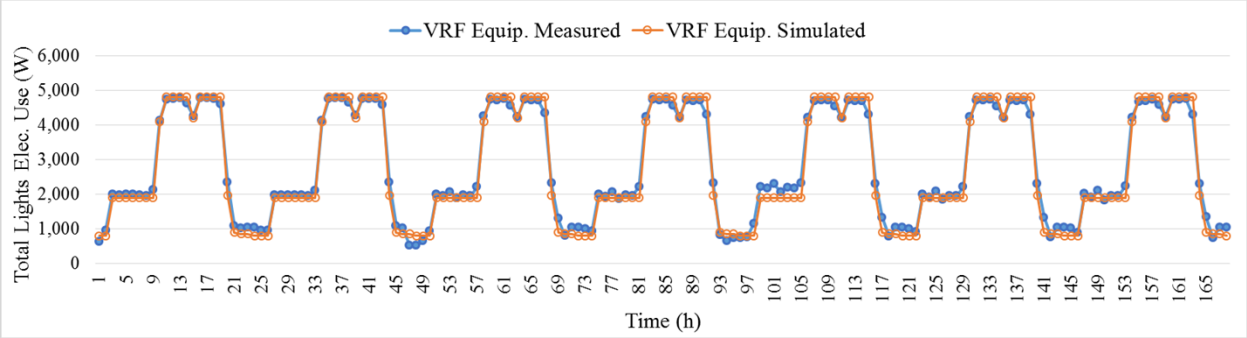

Figure 10. Hourly interior equipment electricity use for typical seven days

After updating the building envelope model, Delivered cooling and heating loads are compared to the simulated values. System delivered loads are calculated by Eq. (1), where $\dot{m}_a$, h_{return}, and h_{supply} are the mass flow rate of dry air through heating and cooling coils, return air enthalpy, and supply air enthalpy, respectively.

$$Load_{Delivered} = \dot{m}_a \times (h_{return} - h_{supply}) \quad (1)$$

3.3 Step 3: Calibration 2 – VRF-DOAS system

The VRF-DOAS model is also calibrated after the building load calibration. The calibrated building load model in Step 2 is used to calibrate the VRF-DOAS simulation model based on the measured data from the FRP. The following items are added and modified in the VRF calibration process:

1) DOAS using the modified version of EnergyPlus 8.1
2) DOAS outdoor air (OA) set point temperature
3) VRF operation schedule

4) Heating and cooling COPs of the VRF system

An air-loop DOAS is implemented in the VRF simulation model using the modified version of EnergyPlus 8.1 as described in step 1, based on the specifications of the installed DOAS in the FRP. As illustrated in Figure 2, this implementation allows for OA to be provided through an air-loop DOAS directly to individual zones. With the DOAS, OA can be conditioned with VRF heating and cooling coils that are connected to the VRF outdoor unit for the zonal VRF indoor units.

The DOAS schedule and the OA supply air temperature set point are determined based on the measured data for the VRF system in the FRP. The DOAS operation in the model is controlled by an energy management system (EMS) object. The DOAS is always turned on during all hours in summer, but it is operated only during occupied hours during heating season (December–March).

The VRF operation schedule is then modified according to the actual VRF system operation. Since the VRF system installed in the FRP cannot provide simultaneous cooling and heating, the VRF cooling and heating operation schedules are specified separately for the cooling (April–November) and heating (December–March) period, which is the same case for actual operation schedule of the VRF system. The thermostat set point temperature and schedule are set to 24°C and 21.1°C for cooling and heating during occupied hours, respectively.

Finally, the heating and cooling COPs of the VRF model are modified based on the actual performance of the VRF system in the FRP, which were observed from the measured data. The nominal COP values used for the cooling and heating coils were set to 3.0 and 2.5, respectively.

3.4 Graphical and statistical evaluations of a VRF-DOAS simulation model

As a final step of the calibration, the measured and the simulated data are compared to calibrate the whole building simulation model using graphical and statistical comparison techniques. ASHRAE Guideline 14 [42] is used to evaluate the validity of the calibrated models. With this guideline, hourly load and end-use energy profiles represent the hourly fit for the measured versus the simulated data since the graphical analysis includes the time period comparison. In addition, both the simulated and the measured loads and energy consumption are plotted versus the OA temperature to illustrate the relationship between these variables.

For statistical evaluation, two calibration criteria, the Normalized Mean Bias Error (NMBE) and Coefficient of Variation of Root Mean Square Error (CV-RMSE), are used to determine how well a simulation model fits with the measure data. CV-RMSE and NMBE are calculated by Eq. (2) and (3), where s_i, m_i, and $\overline{m}$ represent the simulated results, the measured data, and the average measured data at instance i with p=1, respectively. It states that models are declared to be calibrated if they produce NMBE within ± 10% and CV-RMSE within ± 30% when hourly data are used, or 5% and 15%, respectively, with monthly data.

$$CV(RMSE) = 100 \times \frac{\sqrt{\left(\sum_{i=1}^{n}(m_i - s_i)^2/(n-p)\right)}}{\overline{m}} \tag{2}$$

$$NMBE = 100 \times \frac{\sum_{i=1}^{n}(m_i - s_i)}{(n-p) \times \overline{m}} \tag{3}$$

4. DISCUSSION AND RESULTS ANALYSIS

4.1 Comparison of the total VRF-DOAS delivered load

The hourly total delivered load of the VRF-DOAS system is compared against the measured data from the FRP during operation period, from August 2015 through February 2016. Figure 11 shows the hourly profile of the simulated VRF-DOAS delivered load compared with the calculated results using Eq. (1). Positive and negative ranges of the delivered load indicate cooling and heating loads, respectively. From the hourly comparative patterns shown in Figure 11, the comparable results illustrate good agreement between the simulated and the measured data in most hours; however, the hourly data reveal that the simulation model often under-predict the high delivered load required in the beginning of system start-up in the morning for cooling period. This can be caused by various sources of uncertainty in a building performance simulation process [32], including the uncertainty of thermal mass and material properties for the building envelope model, or model algorithm itself.

Figure 12 represents the scatter-plots of the hourly delivered load of VRF-DOAS model as a function of hourly average OA temperature during occupied hours. The simulated delivered load of the VRF-DOAS are compared with the measured data. As seen in this figure, the comparison shows that the simulated delivered load for the VRF-DOAS system are reasonably matched after building components' updates with a NMBE of 3.8%. This calibration step ensures that simulated building loads (envelope + internal gains) match delivered cooling and heating loads, which would be a prerequisite to the HVAC system and control calibration.

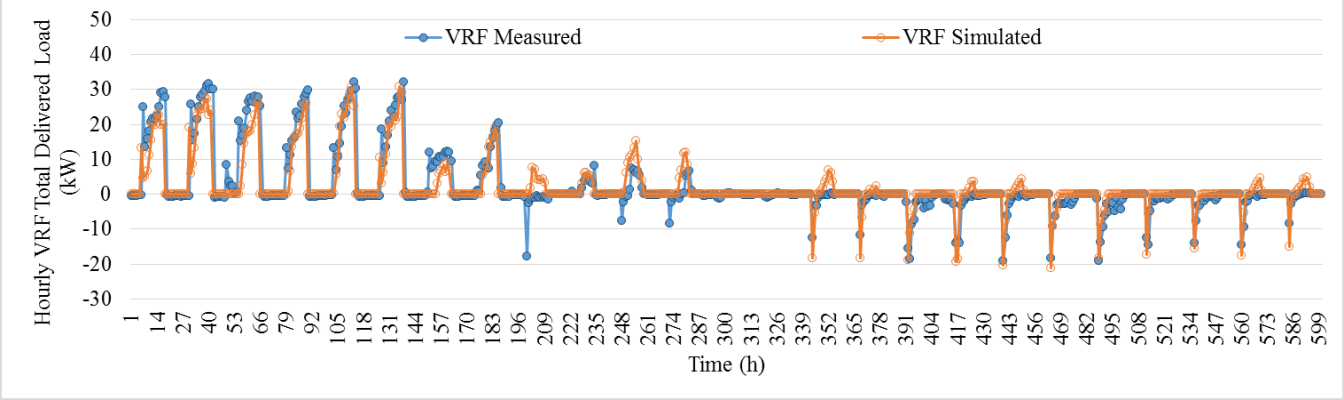

Figure 11. Hourly comparison of the VRF total delivered load between the measured and the simulated data

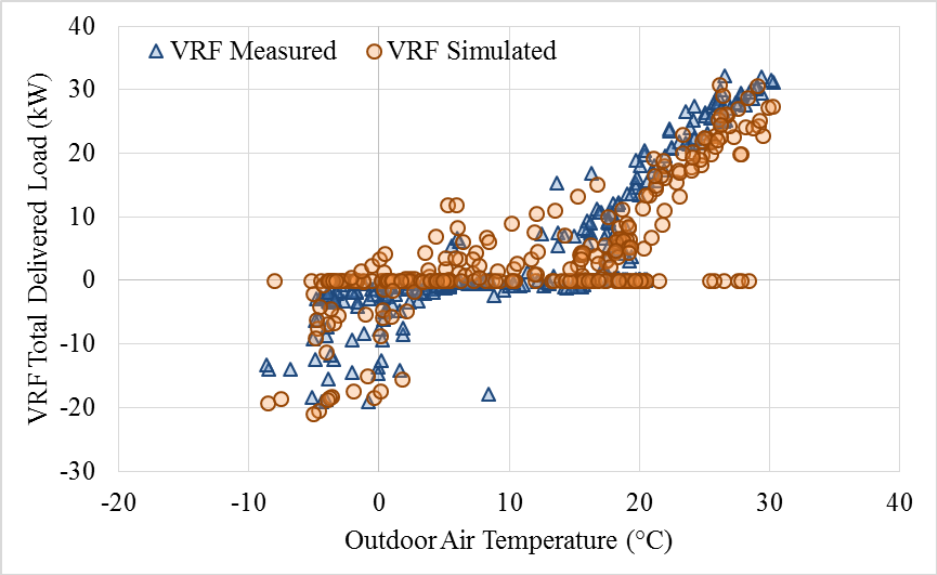

Figure 12. The measured versus the simulated hourly VRF Total delivered load

4.2 Comparison of the DOAS delivered load

Figure 13 shows hourly comparison of the DOAS delivered loads between the simulated and the measured data for operation period. Those values are only driven from the DOAS unit in the VRF-DOAS system and calculated using Eq. (1). In this calculation, h_{return} and h_{supply} are OA inlet air enthalpy and supply air enthalpy passed through the DOAS unit, respectively. As seen in Figure 13, hourly comparison between the simulated and the measured data shows a close match in most hours with a NMBE of 6.4%.

Figure 14. The measured versus the simulated hourly DOAS delivered loadFigure 14 illustrates the scatter-plots of the results, comparing the hourly delivered loads for the measured versus the simulated data as a function of hourly average OA temperature during the occupied hours. As expected, this comparison reveals that the simulated delivered load through the DOAS unit are also well matched after building components and several DOAS unit updates, such as OA operation schedules and supply set-point temperature. Once the input parameters of the simulation modeling are calibrated with the measured data responding to the realistic building and the DOAS unit combined with the VRF system, the effect of specific parameters on the VRF-DOAS can be effectively detected. Therefore, the next calibration step is performed by updating several input parameters (e.g., VRF operation schedule and heating and cooling COP values of the VRF-DOAS) based on compared results for the delivered load.

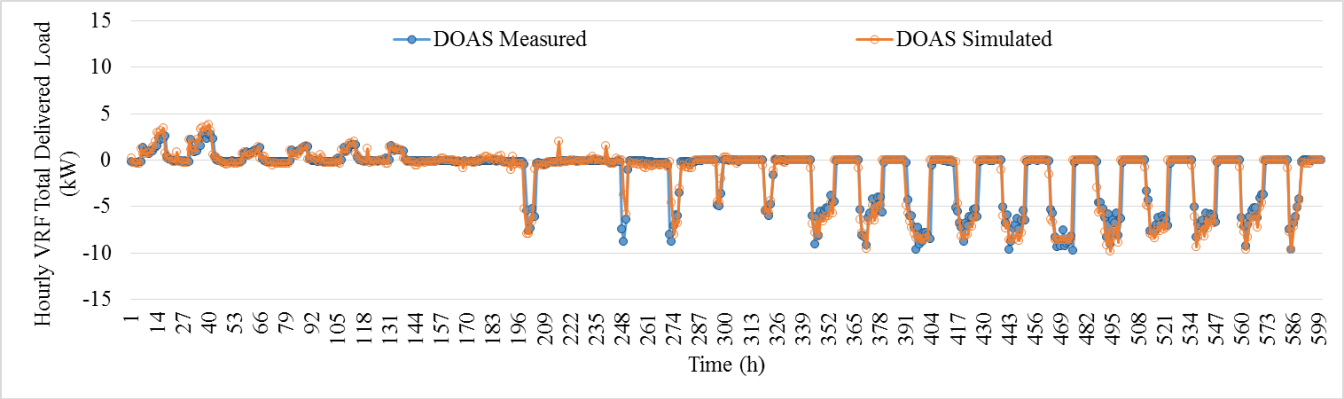

Figure 13. Hourly comparison of the DOAS delivered load between the measured and the simulated data

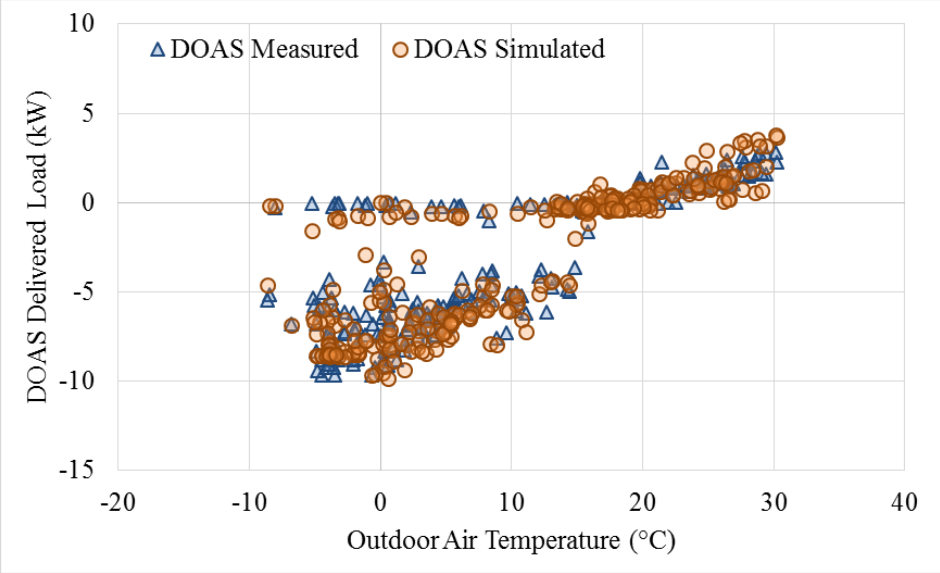

Figure 14. The measured versus the simulated hourly DOAS delivered load

4.3 Comparison of HVAC and whole-building energy use

The simulated building energy use is compared against the measured data after the DOAS unit and VRF system updates. Figure 15 and Figure 16 show the hourly patterns of the simulated VRF-DOAS system and whole-building energy usage compared to the measured energy consumption in the FRP for operation days, from August 2015 through February 2016. Although the simulation model often under-predicts the high HVAC energy usage during the system start-up for cooling and transition periods in a similar fashion of the VRF-DOAS delivered load, the simulation results of the calibrated VRF-DOAS model shown in Figure 15 follow the measured data in a reasonable manner in most hours with a NMBE of 11.5%. HVAC energy consumption of the VRF-DOAS model is based on heating, cooling, and fan electric uses. Hourly comparison of the whole-building energy consumption between the measured and the simulated data is illustrated in Figure 16. The whole-building energy usage typically reflects all electrical consumption used for interior lights, equipment, and HVAC energy usage in the FRP.

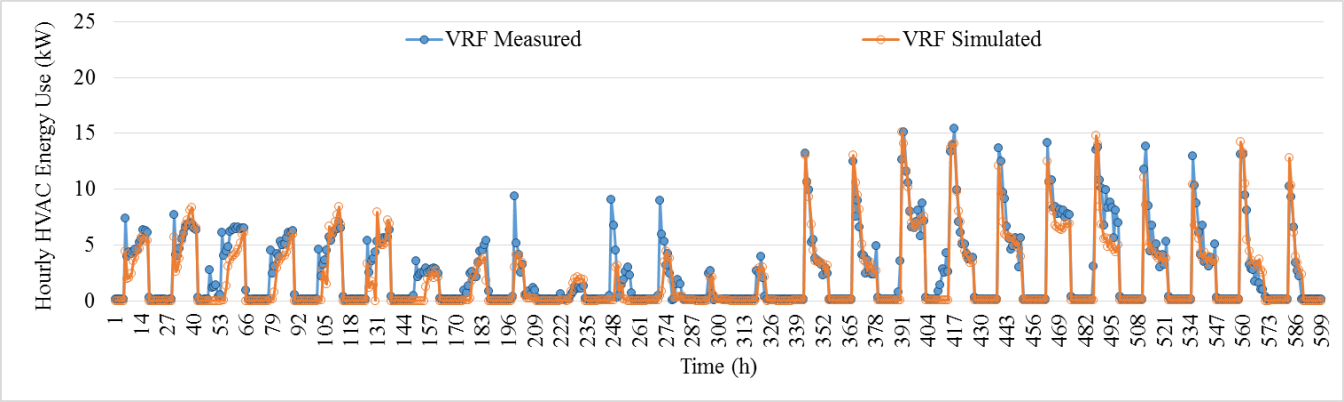

Figure 15. Hourly comparison of HVAC energy use between the measured and the simulated data

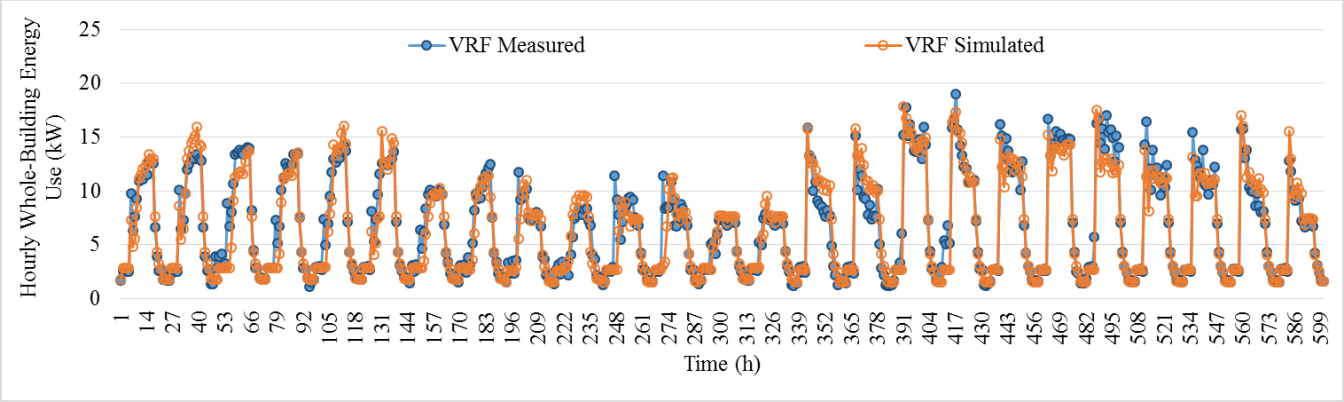

Figure 16. Hourly comparison of the whole-building energy use between the measured and the simulated data

Figure 17 and Figure 18 show scatter-plots of the simulated hourly VRF-DOAS system and the whole-building energy usage with the measured data versus hourly average OA temperature during the entire cooling and heating period. The VRF-DOAS is operated by a master thermostat, which is located in room 106 on the first floor to determine heating or cooling mode. Figure 17 (a) and Figure 18 (a) compare the measured data and the uncalibrated simulated data for hourly HVAC and whole-building energy consumption respectively. As expected, it is observed that there are significant errors when the initial building energy model is uncalibrated.

After the proper calibration with the measured data throughout all steps, the simulation results from the calibrated VRF-DOAS model fit reasonably well with the measured data. In a similar fashion to Figure 17 (b), Figure 18 (b) illustrates a scatter-plot of the measured and the simulated data versus hourly OA temperature for the calibrated whole-building energy consumption. It agrees reasonably well with the measured data in the cooling and the heating operation.

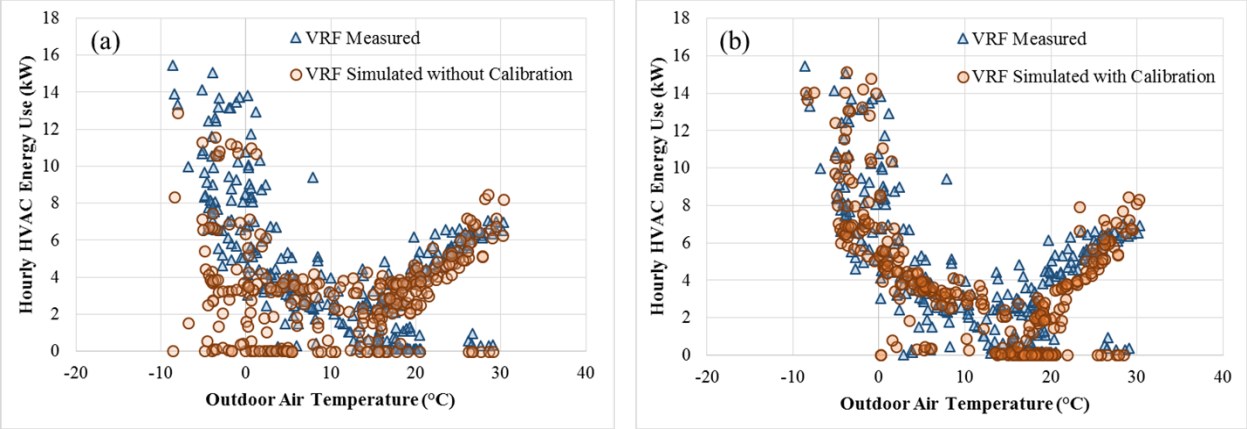

Figure 17. The measured versus the simulated hourly HVAC system energy use during the entire comparative period: (a) without calibration and (b) with calibration

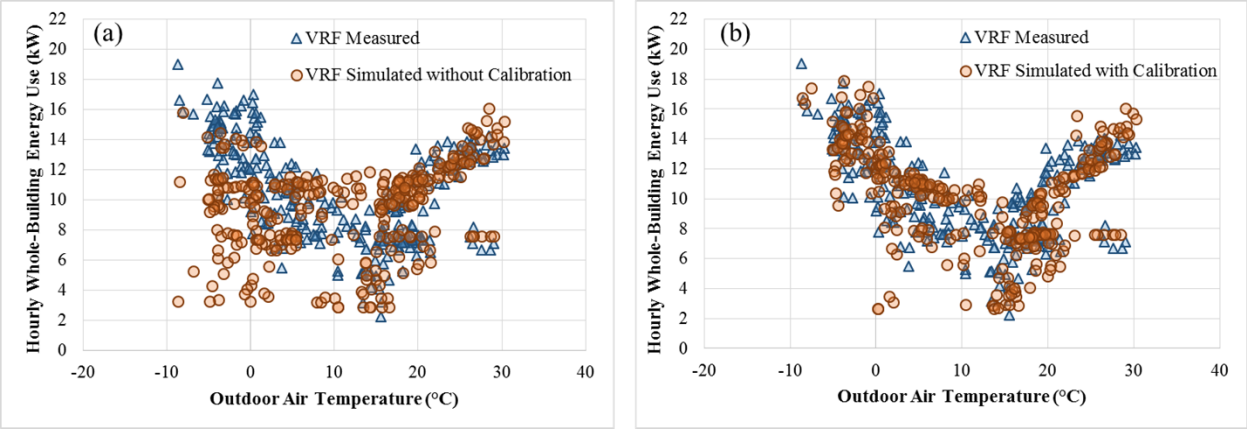

Figure 18. The measured versus the simulated hourly total energy use during the entire comparative period: (a) without calibration and (b) with calibration

4.4 Comparison of statistical evaluation for the simulated and the measured results

Figure 19 illustrates how the simulated data of daily building energy usage compares with the measured data. From the perspective of the coefficients of determination (R^2) shown in Figure 19, a strong correlation ($R^2 = 0.8615$) between the simulated and the measured whole-building energy use is observed with a detailed calibration for daily scale, while the correlation between the uncalibrated simulated and the measured data is less strong ($R^2 = 0.3104$).

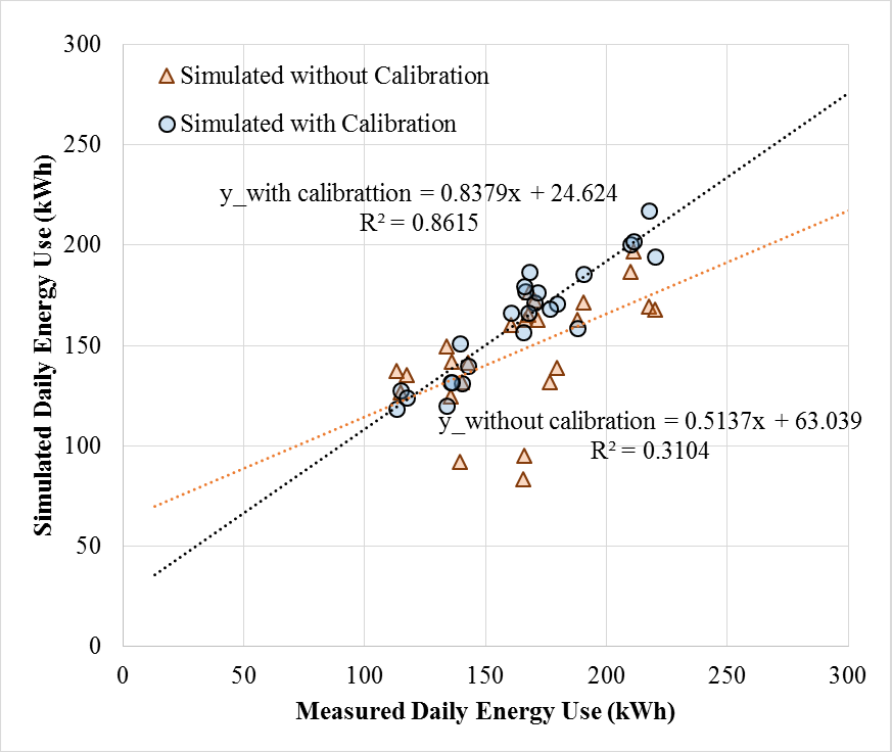

Figure 19. Linear relationship of daily whole building end-use for the measured versus the simulated data

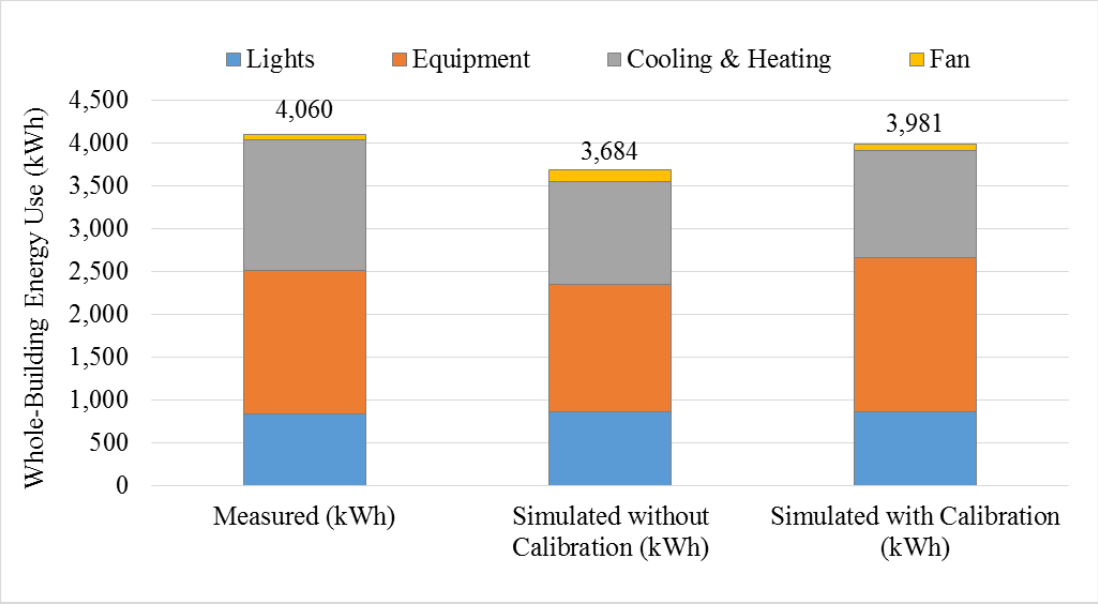

Figure 20. Total comparison of the whole-building energy use of the VRF-DOAS model

Figure 20 shows the whole-building energy use for the uncalibrated and the calibrated results of the VRF-DOAS model, which indicates that the difference in the whole-building energy based on the measured data decreased from 9.3% (376.1 kWh) to 1.9% (78.8 kWh) for the chosen 25 days from August, 2015, through February, 2016.

Table 2 presents the detailed values of building energy consumption among the measured data, the uncalibrated model data and the data after the calibration. The results show that the differences between the measured data to the calibrated data are 8.3% (66.1 kWh) for lights, 7.4% (123.8 kWh) for equipment, 17.9% (272.0 kWh) for cooling and heating systems, and 4.8% (3.3 kWh) for VRF fan. The differences for lights and equipment are due to altered operations of those on some test days from the regular schedules.

Table 2. The whole-building energy use of the VRF-DOAS model

	Lights	**Equip.**	**Cooling & Heating**	**Fan**	**Total**
Measured [kWh]	795.0	1,674.8	1,521.7	68.2	4,059.7
Simulated without calibration [kWh]	864.3	1,483.4	1,203.1	132.8	3,683.6
Simulated with calibration [kWh]	861.1	1,798.6	1,249.7	71.5	3,980.9
Diff. without calibration [%]	8.7%	11.4%	20.9%	94.6%	9.3%
Diff. with calibration [%]	8.3%	7.4%	17.9%	4.8%	1.9%

Table 3 summarizes the CV-RMSE and NMBE for the uncalibrated and calibrated whole building models. The calculated analysis results, based on the whole-building energy consumption (i.e., interior lights, equipment, and HVAC electric uses), are reasonably calibrated based on the criteria from the ASHRAE Guideline 14-2014. The calculated results indicate that CV-RMSE and NMBE for hourly data are 15.7% and 3.8%, respectively, after the proper calibration, which are all within the acceptable criteria ranges. For daily comparison, CV-RMSE and NMBE are 8.7% and 0.2%, respectively, after the calibration.

Table 3. Statistical evaluation of the whole building models

		Without calibration (%)	**With calibration (%)**
Daily	CV-RMSE	20.1	8.7
	NMBE	9.6	0.2
Hourly	CV-RMSE	32.3	15.7
	NMBE	10.9	3.8

5. CONCLUSION

Modeling and calibration of a VRF system with a DOAS is performed using the modified EnergyPlus program based on the measured data from the FRP. Energy consumption and properties (e.g., temperature and air flow rate) at each unit of the VRF-DOAS are measured for 25 days during cooling and heating periods. The calibration processes in three main stages: (1) VRF-DOAS source code modification of EnergyPlus 8.1, (2) building load calibration, and (3) VRF-DOAS system updates for final calibration until

the statistical comparison shows acceptable match under the criteria defined in the ASHRAE Guideline 14-2014.

The calibration results show that hourly CV-RMSE and NMBE would be within 15.7% and 3.8%, while an uncalibrated model error is about 32.3% and 10.9% for hourly CV-RMSE and NMBE, respectively. The results also show that the whole-building energy usage after a detailed calibration of the VRF-DOAS model is 1.9% (78.8 kWh) lower than that of the measurements during comparison period. These results indicate that after the proper calibration with detailed monitored building performance data, the heat pump type VRF-DOAS model can reasonably predict the performance of the actual VRF system under the criteria defined in ASHRAE Guideline 14-2014. In addition, it would be preferred to calibrate the simulated building envelope load with the DOAS unit before performing HVAC system level calibration whenever it is possible.

Based on this study, future research should include the investigation of proper control strategies to reduce HVAC energy consumption with maintaining good indoor air quality (IAQ). In addition, calibration analysis to evaluate energy performance of VRF systems should be considered using heat recovery (HR) modes and actual performance curves of recent VRF systems from the manufacturer data.

ACKNOWLEDGEMENT

This manuscript has been authored by UT-Battelle, LLC, under Contract Number DEAC05-00OR22725 with DOE. The United States Government retains and the publisher, by accepting the article for publication, acknowledges that the United States Government retains a non-exclusive, paid-up, irrevocable, world-wide license to publish or reproduce the published form of this manuscript, or allow others to do so, for United States Government purposes.

REFERENCE

[1] EIA, “Energy Consumption by Sector,” *Energy*, 2015. [Online]. Available: http://www.eia.gov/totalenergy/data/monthly/pdf/sec2_3.pdf. [Accessed: 01-Jan-2016].

[2] K. J. Chua, S. K. Chou, W. M. Yang, and J. Yan, “Achieving better energy-efficient air conditioning - A review of technologies and strategies,” *Appl. Energy*, vol. 104, pp. 87–104, 2013.

[3] W. Goetzler, “Variable Refrigerant Flow Systems,” *ASHRAE J.*, vol. 49, no. 4, pp. 24–31, 2007.

[4] A. Amarnath and M. Blatt, “Variable Refrigerant Flow : An Emerging Air Conditioner and Heat Pump Technology Evolution of the Technology,” *ACEEE Summer Study Energy Effic. Build.*, pp. 1–13, 2008.

[5] K. W. Roth, J. Dieckmann, S. D. Hamilton, and W. Goetzler, “Energy Consumption Characteristics of Commercial Building HVAC Systems Volume III : Energy Savings Potential,” *Build. Technol. Progr.*, vol. III, no. 68370, 2002.

[6] P. Im, J. D. Munk, and A. C. Gehl, *Evaluation of Variable Refrigerant Flow Systems Performance and the Enhanced Control Algorithm on Oak Ridge National Laboratory’s Flexible Research Platform*. Oak Ridge, TN: Oak Ridge National Laboratory (ORNL), 2015.

[7] T. N. Aynur, “Variable refrigerant flow systems: A review,” *Energy Build.*, vol. 42, no. 7, pp. 1106–1112, 2010.

[8] P. Im and J. D. Munk, “Evaluation of Variable Refrigerant Flow (VRF) System Performance Using an Occupancy Simulated Research Building : Introduction and Summer Data Analysis Compared with a Baseline RTU System,” *ASHRAE Annu. Conf.*, pp. 1–9, 2015.

[9] D. Kim, S. J. Cox, H. Cho, and P. Im, “Evaluation of energy saving potential of variable refrigerant flow (VRF) systems compared with variable air volume (VAV) systems in the U.S. climate locations,” *Proc. 3rd Aisa Conf. Int. Build. Perform. Simul. Assoc.*, vol. 3, pp. 85–93,

2017.
[10] Y. P. Zhou, J. Y. Wu, R. Z. Wang, and S. Shiochi, “Energy simulation in the variable refrigerant flow air-conditioning system under cooling conditions,” *Energy Build.*, vol. 39, no. 2, pp. 212–220, 2007.
[11] X. Yu, D. Yan, K. Sun, T. Hong, and D. Zhu, “Comparative study of the cooling energy performance of variable refrigerant flow systems and variable air volume systems in office buildings,” *Appl. Energy*, vol. 183, pp. 725–736, 2016.
[12] T. N. Aynur, Y. Hwang, and R. Radermacher, “Simulation comparison of VAV and VRF air conditioning systems in an existing building for the cooling season,” *Energy Build.*, vol. 41, no. 11, pp. 1143–1150, 2009.
[13] J. Meng, M. Liu, W. Zhang, R. Cao, Y. Li, H. Zhang, X. Gu, Y. Du, and Y. Geng, “Experimental investigation on cooling performance of multi-split variable refrigerant flow system with microchannel condenser under part load conditions,” *Appl. Therm. Eng.*, vol. 81, pp. 232–241, 2015.
[14] J. M. Choi and Y. C. Kim, “Capacity modulation of an inverter-driven multi-air conditioner using electronic expansion valves,” *Energy*, vol. 28, no. 2, pp. 141–155, 2003.
[15] Y. Zhu, X. Jin, Z. Du, B. Fan, and S. Fu, “Generic simulation model of multi-evaporator variable refrigerant flow air conditioning system for control analysis,” *Int. J. Refrig.*, vol. 36, no. 6, pp. 1602–1615, 2013.
[16] T. N. Aynur, Y. Hwang, and R. Radermacher, “Integration of variable refrigerant flow and heat pump desiccant systems for the cooling season,” *Appl. Therm. Eng.*, vol. 30, no. 8–9, pp. 917–927, 2010.
[17] Y. Jiang, T. Ge, and R. Wang, “Performance simulation of a joint solid desiccant heat pump and variable refrigerant flow air conditioning system in EnergyPlus,” *Energy Build.*, vol. 65, pp. 220–230, 2013.
[18] Q. Tu, D. Zou, C. Deng, J. Zhang, L. Hou, M. Yang, G. Nong, and Y. Feng, “Investigation on output capacity control strategy of variable refrigerant flow air conditioning system with multi-compressor,” *Appl. Therm. Eng.*, vol. 99, pp. 280–290, 2016.
[19] ASHRAE, “ANSI/ASHRAE Standard 62.1-2013-Ventilation for Acceptable Indoor Air Quality,” Atlanta, 2013.
[20] W. Kim, S. W. Jeon, and Y. Kim, “Model-based multi-objective optimal control of a VRF (variable refrigerant flow) combined system with DOAS (dedicated outdoor air system) using genetic algorithm under heating conditions,” *Energy*, vol. 107, pp. 196–204, 2016.
[21] Y. Zhu, X. Jin, Z. Du, X. Fang, and B. Fan, “Simulation of variable refrigerant flow air conditioning system in heating mode combined with outdoor air processing unit,” *Energy Build.*, vol. 68, no. 1–2, pp. 571–579, 2014.
[22] T. N. Aynur, Y. Hwang, and R. Radermacher, “The Effect of the Ventilation and the Control Mode on the Performance of a VRV System in Cooling and Heating Modes,” in *International Refrigeration and Air Conditioning Conference*, 2008, vol. 14, no. 5, pp. 783–795.
[23] Y. Li, J. Wu, and S. Shiochi, “Modeling and energy simulation of the variable refrigerant flow air conditioning system with water-cooled condenser under cooling conditions,” *Energy Build.*, vol. 41, no. 9, pp. 949–957, 2009.
[24] Y. M. Li, J. Y. Wu, and S. Shiochi, “Experimental validation of the simulation module of the water-cooled variable refrigerant flow system under cooling operation,” *Appl. Energy*, vol. 87, no. 5, pp. 1513–1521, 2010.
[25] B. Shen, C. K. Rice, T. P. Mcdowell, and V. D. Baxter, “Energy Simulation of Integrated Multiple- Zone Variable Refrigerant Flow System,” in *ASHRAE Annual Conference*, 2013.
[26] R. Raustad, “A variable refrigerant flow heat pump computer model in energyplus,” *ASHRAE Trans.*, vol. 119, no. PART 1, pp. 299–308, 2013.
[27] C. Sharma and R. Raustad, “Compare Energy Use in Variable Refrigerant Flow Heat Pumps Field Demostration and Compter Model,” in *ASHRAE Annual Conference*, 2013.

[28] T. Hong, K. Sun, R. Zhang, R. Hinokuma, S. Kasahara, and Y. Yura, "Development and validation of a new variable refrigerant flow system model in EnergyPlus," *Energy Build.*, vol. 117, pp. 399–411, 2016.
[29] S. Reddy, B. Hunn, and D. Hood, "Determination of retrofit savings using a calibrated building energy simulation model," *Proc. 9th Symp. Improv. Build. Syst. Hot Humid Clim.*, p. 153–165., 1994.
[30] T. Agami Reddy, "Literature Review on Calibration of Building Energy Simulation Programs," *ASHRAE Trans.*, vol. 112, no. 1, pp. 226–240, 2006.
[31] J. A. Clarke, P. . Strachan, and C. Pernot, "An approach to the calibration of building energy simulation models," *ASHRAE Trans.*, 1993.
[32] D. Coakley, P. Raftery, and M. Keane, "A review of methods to match building energy simulation models to measured data," *Renew. Sustain. Energy Rev.*, vol. 37, pp. 123–141, 2014.
[33] P. Raftery, M. Keane, and J. O. Donnell, "Calibrating whole building energy models : An evidence-based methodology," *Energy Build.*, vol. 43, no. 9, pp. 2356–2364, 2011.
[34] M. Liu, G. Wei, and D. Claridge, "Calibrating AHU Models Using Whole Building Cooling and Heating Energy Consumption Data," *Proc. ACEEE 1998 Summer Study Energy Effic. Build.*, vol. 3, pp. 229–241, 1998.
[35] J. Yoon, E. J. Lee, and D. E. Claridge, "Calibration Procedure for Energy Performance Simulation of a Commercial Building," *J. Sol. Energy Eng.*, vol. 125, no. 3, p. 251, 2003.
[36] M. Royapoor and T. Roskilly, "Building model calibration using energy and environmental data," *Energy Build.*, vol. 94, pp. 109–120, 2015.
[37] Y. J. Kim and C. S. Park, "Stepwise deterministic and stochastic calibration of an energy simulation model for an existing building," *Energy Build.*, vol. 133, pp. 455–468, 2016.
[38] G. Mustafaraj, D. Marini, A. Costa, and M. Keane, "Model calibration for building energy efficiency simulation," *Appl. Energy*, vol. 130, pp. 72–85, 2014.
[39] K. Sun, T. Hong, S. C. Taylor-lange, and M. A. Piette, "A pattern-based automated approach to building energy model calibration," *Appl. Energy*, vol. 165, pp. 214–224, 2016.
[40] B. Shen and C. K. Rice, "Multiple-zone variable refrigerant flow system modeling and equipment performance mapping," *ASHRAE Trans.*, vol. 118, no. PART 1, pp. 420–427, 2012.
[41] G. Y. Yun and K. Song, "Development of an automatic calibration method of a VRF energy model for the design of energy efficient buildings," *Energy Build.*, vol. 135, pp. 156–165, 2017.
[42] ASHRAE, "ANSI/ASHRAE Guideline 14-2014 Measurement of Energy and Demand Savings," Atlanta, 2014.
[43] H. Rutkowski, *Commercial Load Calculation for Small Commercial Buildings*, 5th ed. Air Conditioning Contractors of America, 2008.
[44] DOE, "EnergyPlus Engineering Reference: The Reference to EnergyPlus Calculations, Version 8.1," 2013.
[45] DOE, "EnergyPlus Input Output Reference: the encyclopedic reference to EnergyPlus input and output, version 8.1," 2013.
[46] K. Gowri, D. Winiarski, and R. Jarnagin, "Infiltration Modeling Guidelines for Commercial Building Energy Analysis," *Contract*, no. September, p. 21, 2009.